# How Crystals Nucleate and Grow in Aqueous NaCl Solution

Debashree Chakraborty and G. N. Patey*

Department of Chemistry, University of British Columbia, Vancouver, British Columbia, Canada V6T 1Z1

ABSTRACT: Large-scale molecular dynamics simulations (64 000 particles) are used to examine the microscopic mechanism of crystal nucleation and growth in a slightly supersaturated solution of NaCl in water at 300 K and 1 atm. Early-stage nucleation is observed, and the growth of a single crystal is followed for ~140 ns. It is shown that the nucleation and growth process is better described by Ostwald's rule of stages than by classical nucleation theory. Crystal nucleation originates in a region where the local salt concentration exceeds that of the bulk solution. The early-stage nucleus is a loosely ordered arrangement of ions that retains a significant amount of water. The residual water is slowly removed as the crystal grows and evolves toward its stable anhydrous state.
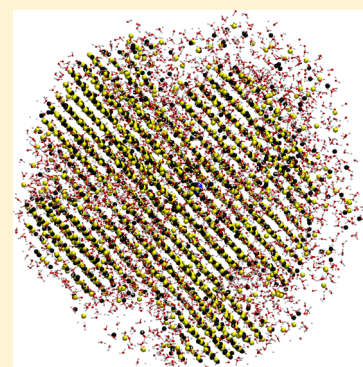
SECTION: Liquids; Chemical and Dynamical Processes in Solution

Crystal nucleation and growth both from melts and solution is of obvious importance in a great variety of physical systems and situations.[1-3] There has been a good deal of recent interest in the microscopic nature of crystallization, with particular focus on the initial stages. The central question is whether classical nucleation theory (CNT),[1-3] the Ostwald rule of stages,[4,5] or some other nucleation mechanism applies. CNT assumes that the initial nucleus is simply a smaller version of the stable bulk crystal phase, such that the nucleation barrier is determined by competition between the favorable free-energy difference between the crystal and solution phases and the inhibiting crystal−solution interfacial tension. In this picture, at some critical size, the bulk free-energy difference prevails, and the nucleus grows to form a macroscopic crystal. Unlike CNT, the Ostwald rule does not assume that the nucleus is necessarily closely related to the stable bulk crystal phase but rather that the initial nucleus is more likely to be some metastable structure closer in free energy to the solution phase from which it is emerging. The thermodynamically stable crystal then develops from this nucleus through "stages" as the system evolves toward equilibrium.

The early stages of crystallization are difficult to identify and follow experimentally, but recent detailed work on colloidal suspensions,[6,7] protein solutions,[8] and, in one case, an inorganic salt[9,10] tend to support the Ostwald picture rather than the CNT mechanism. There have also been a number of computer simulation studies of crystal nucleation in systems modeled using variations of hard-sphere[11,12] and soft-sphere[13-16] potentials. Although the nucleation mechanisms that emerge from these investigations differ in detail, sometimes substantially so, the overall picture is strongly supportive of Ostwald's idea of stepwise nucleation and growth processes. This is also consistent with a recent theoretical analysis employing density functional methods.[17]

There have been efforts to investigate nucleation and crystal growth in salt solutions,[3,18,19] with particular attention focused on aqueous NaCl systems.[18-23] It is possible with direct molecular dynamics (MD) simulations to observe crystallization, or at least the formation of large ordered clusters, in supersaturated salt water solutions.[18,20,22,23] However, to date, direct simulations of NaCl crystallization have been confined to relatively small samples, and the mechanism of crystal growth over time has not been examined in detail. Additionally, it is uncertain how closely small systems can represent crystal growth in the macroscopic limit, where, at equilibrium, the salt crystal must coexist with saturated solution. In small supersaturated systems, most ions tend to associate into a cluster, with few (if any) remaining free in solution. Very early stage nucleation in salt solutions has also been considered for small systems employing path sampling techniques,[21] and another indirect method for following crystal growth has been proposed[19] but, as discussed by the authors, is not useful for highly soluble salts such as sodium chloride.

In the present Letter, we employ direct, large-scale MD simulations to examine crystal nucleation and growth in NaCl solution. We consider slightly supersaturated conditions such that ~7 ns are required to observe crystal nucleation. This is advantageous because it allows us to clearly identify our initial condition as a well "equilibrated" metastable solution. Moreover, under these conditions, we observe only a single crystal nucleate and grow, which permits us to follow a specific well-defined process. In highly supersaturated solutions, the situation is complicated by the rapid nucleation of multiple crystals that grow, interact, and sometimes combine as the

system evolves in time. The growth and interaction of multiple crystal nuclei raises other interesting questions concerning the evolution to equilibrium of a macroscopic salt sample, but we expect these to involve much slower processes. Here, we follow a single crystal through nucleation and growth up to 150 ns, which is sufficient to give a clear picture of the mechanism. Our most significant finding is that the crystal nucleation and growth follows an Ostwald-like process. A local region of relatively high salt concentration appears prior to discernible spatial ordering, the early-stage salt nucleus contains a significant amount of water, and the anhydrous stable crystal develops slowly as the system evolves in time.

Our simulations were carried out at 300 K and a pressure of 1 atm. The SPC/E model[24] was used for water, and the ion parameters were those used in the OPLS force field.[25,26] All pair interactions consisted of Lennard-Jones (LJ) and Coulombic terms; the relevant LJ parameters and charges are given in Table 1. The LJ cross interactions were obtained using

Table 1. LJ Parameters and Charges for the Models Considered[a]

atom/ion	σ (Å)	ε (kJ/mol)	charge (e)
O	3.166	0.6501	−0.8476
H	0.0	0.0	+0.4238
Na$^+$	3.330	0.0116	+1
Cl$^-$	4.417	0.4928	−1

[a]The O and H parameters are from ref 24, the Na$^+$ parameters are from ref 26, and those for the Cl$^-$ are from ref 25.

the usual Lorentz−Berthelot combining rules.[27] The MD simulations employed GROMACS[28,29] version 4.5.4 in double precision. The equations of motion were integrated using the leapfrog algorithm with a time step of 2 fs. The Coulombic interactions were treated employing the particle mesh Ewald (PME) summation method.[30,31] The simulations were carried out in the *NPT* ensemble, using a velocity rescaling algorithm[32] (τ_t = 0.1 ps) to control the temperature and the Berendsen barostat[33] (τ_p = 0.1 ps) for the pressure. The water molecules were kept rigid by constraining the interatomic distances using the LINCS algorithm.[34] The initial configuration for the simulation was obtained by minimizing the energy of water molecules and ions placed in a cubical box. The system was then equilibrated for 2 ns, followed by a production run of 150 ns. It is important to note that the system was also equilibrated in the sense that the solution properties (energy, radial distribution functions, etc.) were converged and unchanging before crystal nucleation occurred.

In our simulation carried out with 64 000 particles (56 000 water molecules and 4000 ion pairs), crystal nucleation is observed in ~7 ns. (It is perhaps worth mentioning that a 64 000 particle simulation employing 64 cores requires ~7 machine hours for each nanosecond of trajectory.) As noted above, this is a convenient time scale that allows adequate time to equilibrate the metastable solution, giving a well-defined initial state before salt nucleation occurs, but is sufficiently fast that nucleation and crystal growth can be followed with direct MD simulations. The concentration of this solution is 3.97 *m*, and we believe that this is just above the solubility limit for the present model because we could not observe crystal nucleation for concentrations much below this value (3.75 *m*). This concentration (3.97 *m*) is below the solubility limit for real water under these conditions (~6.15 *m*), but it is close to the

saturation concentration (~4.3 *m*) recently reported[35] for a model solution using SPC/E water but employing somewhat different ion interaction parameters. The lower solubility might be at least partially due to the fact that the SPC/E water model has a lower dielectric constant (68) than real water (78.5) under the present conditions.[36] We note that others have recently remarked on the sensitivity of the solubility of NaCl to model parameters.[22,23] While the solubility limit will obviously determine the lowest concentration where nucleation can be observed for a particular model, we would not expect it to strongly influence the mechanism of crystal nucleation and growth.

It is also important to note that near saturation, the time required to observe crystal nucleation can depend rather strongly on system size. For example, in the present case, nucleation is observed in ≲10 ns for 64 000 particles (4000 ion pairs), whereas ~90 ns are required for 8000 particles (500 ion pairs). This difference can be accounted for simply by the larger number of ions in the bigger system and, therefore, a proportionally increased probability of observing nucleation.

A qualitative overview of crystal nucleation and growth in the slightly supersaturated solution is given by the configurational snapshots shown in Figure 1. All 4000 ion pairs are included in
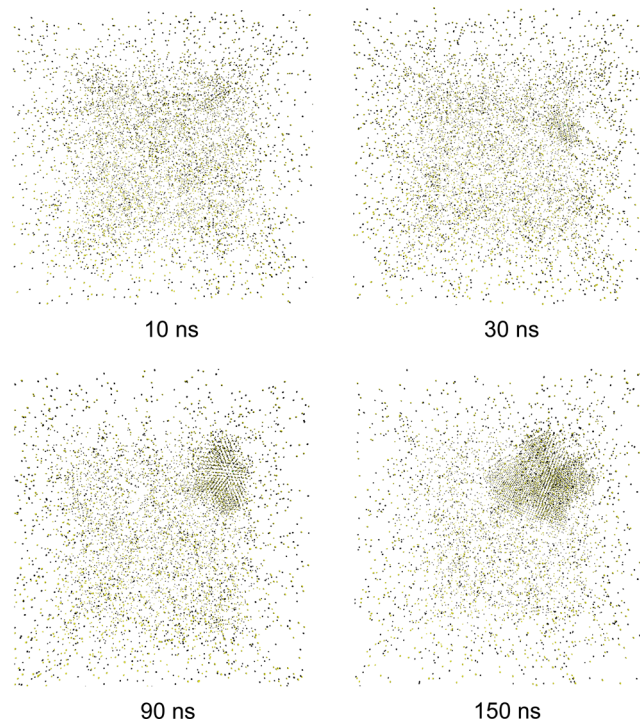

Figure 1. Configurational snapshots showing the crystal growth over time. All Na$^+$ (black) and Cl$^-$ (yellow) ions (not drawn to scale) are shown. The water molecules are omitted for clarity.

the snapshots, but for clarity, the water molecules are not shown. At the magnification level of these snapshots, a growing crystal is apparent at 30 (upper right corner), 90, and 150 ns. A clear crystal structure is not discernible at 10 ns, although we shall show below that nucleation has already occurred at that time. We note that at 3.97 *m*, nucleation and crystal growth is observed only in one location in the system. For higher concentrations (e.g., 5.3 *m*), we observe faster nucleation with crystals growing at multiple sites. However, here, we focus on the lower concentration for the reasons given above.

A more quantitative overview is given in Figure 2, where we have plotted $r^2 h_{+-}(r)$ for times ranging from 10 to 150 ns.
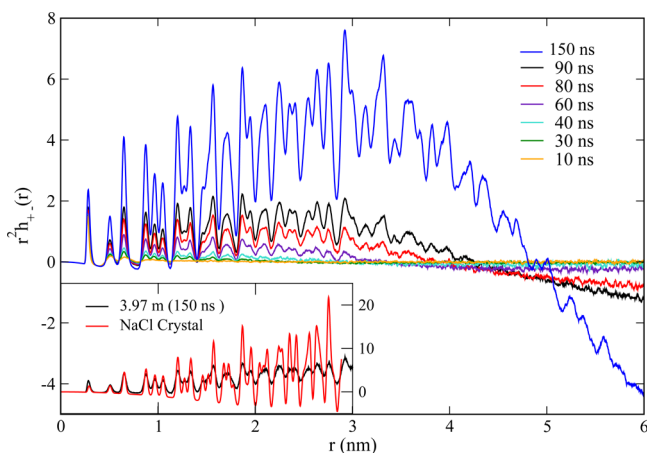

Figure 2. Plots of $r^2 h_{+-}(r)$ showing the growth of crystal structure over time. The inset compares the solution result at 150 ns with that of a pure NaCl crystal at the same temperature and pressure, both normalized to the ion density of the solution. Note that for the inset, the vertical scale is given on the right-hand side.

Here, $h_{+-}(r) = g_{+-}(r) - 1$, where $g_{+-}(r)$ is the $Na^+ - Cl^-$ radial distribution function (rdf), and multiplication by r^2 simply serves to magnify the structural details. We note that $h_{+-}(r)$ is averaged over all ions in the system, whereas only ions in the growing crystal will contribute to the long-range structure. At 10 ns, $r^2 h_{+-}(r)$ is very short ranged and is essentially that of the equilibrated metastable solution. At 30 ns, longer-ranged structural peaks can be discerned in $r^2 h_{+-}(r)$, consistent with the small patch of ordered ions that can be seen in the snapshot at this time (Figure 1). As the NaCl crystal grows in time, the ion–ion correlation increases in range, and the structural peaks become more distinct. The distance where $r^2 h_{+-}(r)$ crosses the axis and becomes negative provides a rough measure of the crystal "size"; the positive region reflects the increase in ion density in the crystal, and the negative region is the corresponding decrease in ion density in the surrounding solution. The inset in Figure 2 compares the solution result at 150 ns with the $r^2 h_{+-}(r)$ obtained by simulating a pure NaCl crystal (4000 ion pairs) at the same temperature and pressure. For comparison purposes, both rdfs are normalized to the ion density of the solution. We note that for $r \lesssim 1$ nm, the solution and crystal results are in close agreement, confirming that at 150 ns, the structure of the interior of the ordered region is very close to that of the anhydrous NaCl crystal. At larger separations, the crystal and solution peaks are in similar positions, but the solution structure is less well resolved, consistent with the crystal defects and water content, evident in snapshots and discussed below.

We next turn to the interesting question of how to detect a potential crystal nucleus and follow its trajectory over time. One approach would be to define some order parameter and use it to detect ordered ion clusters that might serve as crystal nuclei. However, a major problem with this method is that we do not know the relevant order parameter a priori. If CNT were to strictly apply, then one could possibly devise an order parameter based on the NaCl crystal structure. However, if the initial nucleus contains a significant amount of water, as one might expect, then any order parameter based on NaCl alone

might not serve as a useful detector of early-stage nucleation. Therefore, we have used a different approach that does not require any preconception of the nucleation process. The method is as follows. Once a growing crystal can be clearly seen in our sample, we select a particular ion near the crystal center and use the MD trajectory to follow the composition and structure of its immediate environment backward and forward in time. This allows us to observe the "birth" of the crystal and its growth from the perspective of the selected ion. We did this for several ions all located near the center of the crystal existing at 30 ns, and the picture of nucleation and growth that emerges is not sensitive to the particular ion selected as a reference.

Configurational snapshots showing different perspectives of the entire crystalline region existing at 150 ns are shown in Figure 3. The Na^+ ion used as a reference point from which to observe the nucleation and growth is shown enlarged and blue in color near the center of the crystal. The snapshots in Figure 3 show that all ions in the ordered region are part of the same crystal structure. There are obvious defects and some disorder
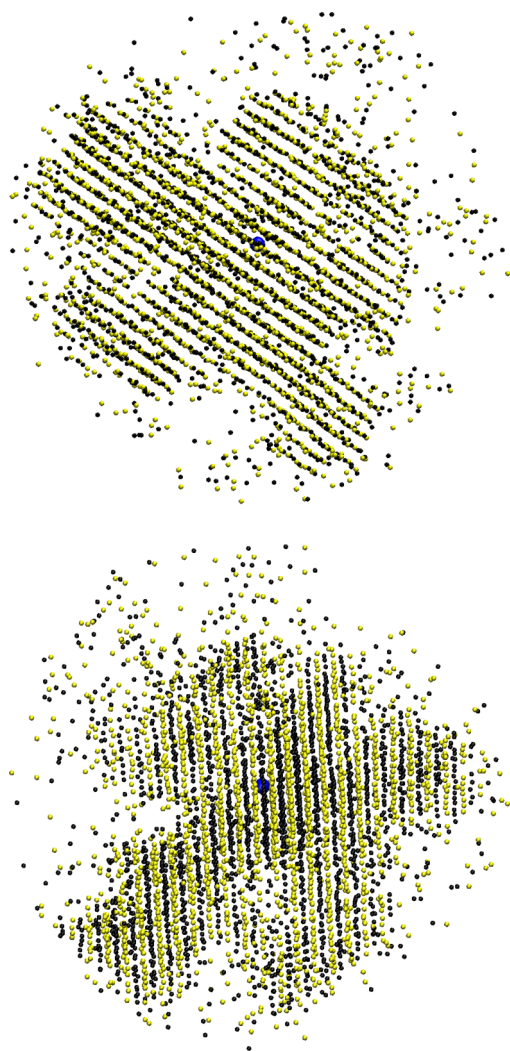

Figure 3. Configurational snapshots showing the entire crystalline region at 150 ns. Na^+ (black) and Cl^- (yellow) ions (not drawn to scale) are shown, but all water molecules are omitted. One selected Na^+ ion near the crystal center is drawn larger and colored blue. This reference ion is used as a position marker in our discussion of crystal nucleation and evolution in time (see text).

near the fringes of the growing crystal, as expected, but the crystal planes are parallel and clearly form a single lattice.

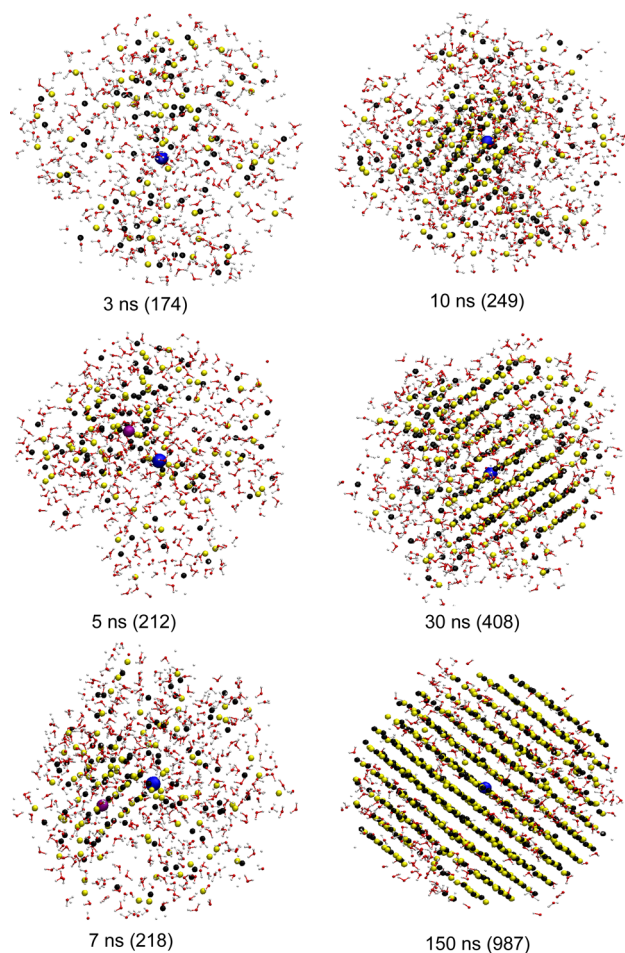Snapshots showing the initiation and growth of the salt crystal are given in Figure 4. Note the central reference Na^+ ion,

Figure 4. Configurational snapshots at different times showing all ions (colors as in Figure 3) within a radius of 2 nm of the reference Na^+ ion (larger and blue). The only water molecules shown (oxygen atoms in red and hydrogen atoms in white) are those within 0.4 nm of at least one of the ions included in the snapshot. Note the marked Cl^- ion (larger and purple) in the 5 and 7 ns snapshots. The numbers given in parentheses are the total number of ions (Na^+ and Cl^-) within 2 nm of the central reference ion.

shown larger and in blue. All ions within 2 nm of this reference ion are shown, and the total number of such ions at each time is given in parentheses in the figure. Only water molecules located within 0.4 nm (approximately within the first coordination shell of a cation or an anion) are shown. Placing this limit on the water molecules included ensures that those appearing in the figure are associated with ions taking part in the crystallization process. From Figure 4, we see that at 3 ns, no order is evident among the ions in the vicinity of the reference ion. At this time, the number of ions within 2 nm of the reference ion is 174, which is just a little above the value (156) obtained by integrating the rdf of the uniform, metastable solution. At 5 ns, the number of ions within 2 nm of the selected ion has increased from 174 to 212, and there is a local region of apparently higher ion density near the selected ion. However, at 5 ns, there is still no clearly discernible ordering of the ions. At

7 ns, the number of ions in the region has increased only slightly (from 212 to 218), but now, some unmistakable crystal-like order has emerged. By marking another ion (a Cl^- shown larger and colored purple) in the 5 and 7 ns snapshots, we confirm that the crystalline order has developed in the denser ion region that can be seen at 5 ns. At 10 ns, the crystal structure can be clearly seen, and the crystalline region grows larger as the system evolves through 30−150 ns (the number of ions in the reference sphere is 249, 408, and 987 at 10, 30, and 150 ns, respectively). We note that by 10 ns, our reference Na^+ ion (enlarged and blue) has become part of the growing crystal.

Thus, the first step in crystal nucleation appears to be the formation of a "collection" of ions that exceeds the bulk concentration but shows little or no spatial order. In the present trajectory, this occurred between 3 and 5 ns. The following step (5−7 ns) involves the development of spatial order, with the local ion density remaining practically constant. Once sufficient local order has developed ($\gtrsim$ 7 ns), the crystalline region grows, acquiring ions from the solution at a relatively rapid rate. We note that these observations appear to be qualitatively consistent with the so-called two-step mechanism of nucleation discussed by Vekilov[8] and others.[17] As formulated by Vekilov,[8] this model suggests that crystal nucleation from solution involves two distinct steps. First, there is a solute "density fluctuation" resulting in a local region of higher solute density (in the present case, a region of higher NaCl concentration); this is followed by a "structure fluctuation" and hence a crystal nucleus. An important feature of this nucleation mechanism is that the density and structure "fluctuations" occur in sequence rather than simultaneously, as assumed by CNT. Our simulations strongly suggest sequential behavior, with a disordered region of high ion concentration serving as a precursor to crystal nucleation.

Another important observation that can be made from the snapshots shown in Figure 4 concerns the role of water in crystal nucleation and growth. The region of high ion density (5 ns) from which the crystal nucleates obviously contains a good deal of water, and the early nucleus (7 ns) is by no means an anhydrous NaCl crystallite. Rather, it is a more loosely ordered arrangement that includes water molecules. The water molecules in the growing nucleus occupy spaces among the ions and do not appear to have any particular order. As time evolves and the crystal grows, its interior becomes "drier", and some anhydrous regions begin to appear. However, the loss of water is a slow process, and some water molecules remain in the interior of the crystalline region even at 150 ns, as can be seen in the snapshot.

The involvement of water in crystal nucleation and growth can be more quantitatively analyzed by calculating ion (including both cations and anions) and water rdfs about the reference Na^+ ion. The rfds obtained at 10, 30, and 150 ns (corresponding to the snapshots in Figure 4) are plotted in Figure 5. Note that these rdfs are obtained from a single configuration at the specified time, which accounts for the larger than usual statistical noise evident in the plots. However, they are accurate enough for our purposes. The crystal growth about the reference ion can be seen in the advancement of the region of high ion density (ion−ion rdf $\gg$ 1) with time. We note that the ion−water rdf within the region of the growing crystal decreases with time as expected, but even at 150 ns, some residual water remains well within the crystal interior. Careful inspection of the ion−water rdfs reveals that the particular Na^+ ion selected as a reference has no first-shell water
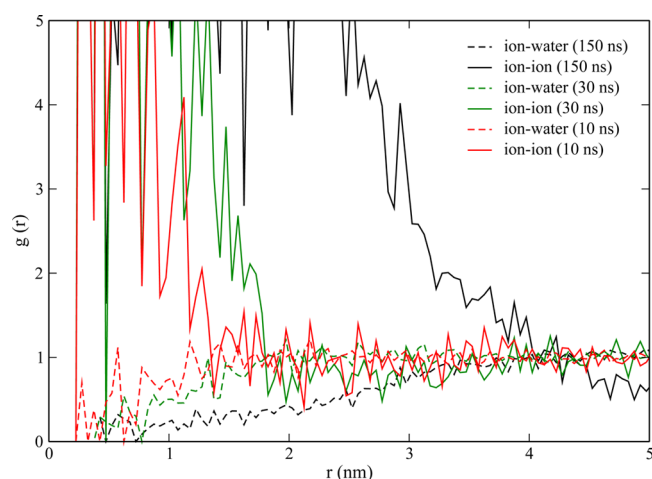
Figure 5. The ion–water and ion–ion (including both Na⁺ and Cl⁻ ions) rdfs about the reference Na⁺ ion shown in Figure 4. Note that each rdf is obtained from the single configuration shown in Figure 4.

of hydration beyond ∼30 ns, but some water molecules persist within ∼0.7 nm of this ion at 150 ns.

We remark that Mucha and Jungwirth[20] have also commented on the role of water in salt crystallization based on their MD simulations of NaCl crystallizing in clusters and slabs from which water is evaporating, detailed results being reported for 900 (cluster) and 500 K (slab). In particular, these authors note that "surface water molecules" facilitate ion rearrangements by lowering potential barriers, hence aiding the crystal growth. This might be related to our observations, but we emphasize that we do not see water molecules involved only at the surface of a growing ion cluster. Rather, in the present case, the water molecules appear to act more as a "component" of the early-stage nucleus.

It is instructive to plot the mole fractions of water molecules and ions located within a fixed radius of the reference ion as a function of time. Results for radii of 1, 1.5, and 2 nm are shown in Figure 6. Focusing on the curves obtained for a radius of 1 nm, we see that between 5 and ∼50 ns, the mole fractions change rapidly as the crystal grows around the reference ion, but beyond ∼50 ns, the curves flatten out and change only very slowly up to 150 ns. This suggests that after nucleation, the
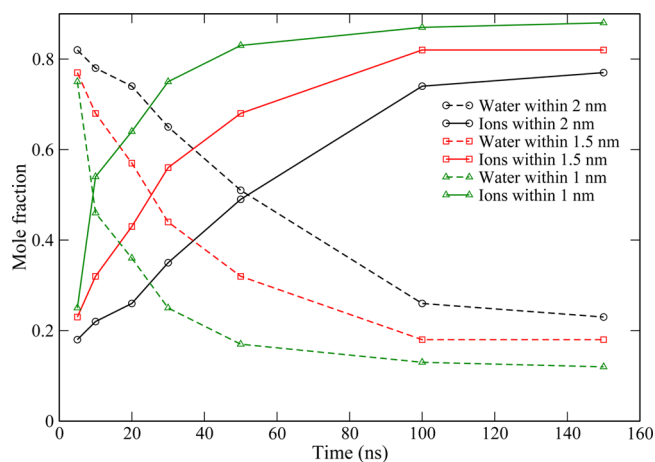
crystal grows rapidly, acquiring ions and excluding water until the reference ion is surrounded by crystal at least 1 nm thick in all directions. However, the crystal formed during this period of rapid growth is not anhydrous and retains ∼18 mol % of residual water within 1 nm of the reference ion. The snapshots suggest that these water molecules tend to reside in "defective" or less ordered regions of the crystal (Figure 4). As the crystal grows larger, the residual water in its interior appears to be slowly excluded, and presumably after some time (long by simulation standards), one would end up with something close to the stable anhydrous state. This pattern is repeated for radii of 1.5 and 2 nm, except that the region of rapid change extends further in time, reflecting the longer times required to grow thicker crystalline layers about the reference ion. The curves in Figure 6, especially their short time behavior, will likely be somewhat sensitive to the exact location of our reference ion and also to the detailed "shape" of the crystal formed in a particular trajectory. However, we would not expect such variations to significantly influence the qualitative physical picture that emerges.

To summarize, our simulation of crystal nucleation and growth in ambient, slightly supersaturated NaCl solution supports Ostwald's rule of stages rather than a CNT-like mechanism. We observe that a disordered region of high local salt concentration forms prior to crystal nucleation. The early-stage nucleus is not a mini crystal of anhydrous NaCl but rather a less ordered arrangement of ions that retains a significant amount of water. From Ostwald's perspective, this is not surprising because we would expect the ion–water composition of the early nucleus to be closer in free energy to the metastable solution than would be the case for an anhydrous NaCl cluster. The residual water appears to be very slowly (on simulation time scales) excluded as the crystal evolves toward its stable anhydrous state.

Finally, it is fair to remark that we have looked in detail only at a single concentration (3.97 m), which is near saturation for the model considered here but lower than the saturation concentration (6.15 m) of a real NaCl solution. Of course, it is always possible that the crystal nucleation and growth mechanism might be sensitive to this concentration difference. However, we have carried out some simulations at a higher concentration (5.3 m), and apart from the formation of multiple crystal nuclei in shorter times, expected due to the increased oversaturation, we did not observe significant differences.

■ AUTHOR INFORMATION

Corresponding Author
*E-mail: patey@chem.ubc.ca.
Notes
The authors declare no competing financial interest.

Figure 6. The mole fractions of water and ions within 1.0, 1.5, and 2.0 nm of the reference Na⁺ ion (Figure 4) as functions of time.

577

dx.doi.org/10.1021/jz302065w | J. Phys. Chem. Lett. 2013, 4, 573–578

■ REFERENCES

(1) De Yoreo, J. J.; Vekilov, P. G. Principles of Crystal Nucleation and Growth. In *Biomineralization*; Dove, P. M., De Yoreo, J. J., Weiner, S., Eds.; Mineralogical Society of America, 54: Washington, DC, 2003; pp 57−93.

(2) Kowacz, M.; Prieto, M.; Putnis, A. Kinetics of Crystal Nucleation in Ionic Solutions: Electrostatics and Hydration Forces. *Geochim. Cosmochim. Acta* **2010**, *74*, 469−481.

(3) Anwar, J.; Zahn, D. Uncovering Molecular Processes in Crystal Nucleation and Growth by Using Molecular Simulation. *Angew. Chem., Int. Ed.* **2011**, *50*, 1996−2013.

(4) Ostwald, W. Studien über die Bildung und Umwandlung fester Körper. *Z. Phys. Chem.* **1897**, *22*, 289−330.

(5) Threlfall, T. Structural and Thermodynamic Explanations of Ostwald'S Rule. *Org. Process Res. Dev.* **2003**, *7*, 1017−1027.

(6) Zhang, T. H.; Liu, X. Y. Multistep Crystal Nucleation: A Kinetic Study Based on Colloidal Crystallization. *J. Phys. Chem. B* **2007**, *111*, 14001−14005.

(7) Zhang, T. H.; Liu, X. Y. Nucleation: What Happens at the Initial Stage? *Angew. Chem., Int. Ed.* **2009**, *48*, 1308−1312.

(8) Vekilov, P. G. Two-Step Mechanism for the Nucleation of Crystals from Solution. *J. Cryst. Growth* **2005**, *275*, 65−76.

(9) Chung, S.-Y.; Kim, Y.-M; Kim, J.-G.; Kim, Y.-J. Multiphase Transformation and Ostwald'S Rule of Stages during Crystallization of a Metal Phosphate. *Nat. Phys.* **2009**, *5*, 68−73.

(10) Billinge, S. J. L. How Do Your Crystals Grow? *Nature Phys.* **2009**, *5*, 13−14.

(11) Lomakin, A.; Asherie, N.; Benedek, G. B. Liquid−Solid Transition in Nuclei of Protein Crystals. *Proc. Natl. Acad. Sci. U.S.A.* **2003**, *100*, 10254−10257.

(12) Auer, S.; Frenkel, D. Numerical Prediction of Absolute Crystallization Rates in Hard Sphere Colloids. *J. Chem. Phys.* **2004**, *120*, 3015−3029.

(13) van Duijneveldt, J. S.; Frenkel, D. Computer Simulation Study of Free Energy Barriers in Crystal Nucleation. *J. Chem. Phys.* **1992**, *96*, 4655−4668.

(14) ten Wolde, P. R.; Frenkel, D. Enhancement of Protein Crystal Nucleation by Critical Density. *Science* **1997**, *277*, 1975−1978.

(15) Anwar, J.; Boateng, P. K. Computer Simulation of Crystallization from Solution. *J. Am. Chem. Soc.* **1998**, *120*, 9600−9604.

(16) Moroni, D.; ten Wolde, P. R.; Bolhuis, P. G. Interplay between Structure and Size in a Critical Nucleus. *Phys. Rev. Lett.* **2005**, *94*, 235703/1−235703/4.

(17) Lutsko, J. F.; Nicolis, G. Theoretical Evidence for a Dense Fluid Precursor to Crystallization. *Phys. Rev. Lett.* **2006**, *96*, 046102/1−046102/4.

(18) Ohtaki, H.; Fukushima, N. Nucleation Processes of NaCl and CsF Crystals from Aqueous Solutions Studied by Molecular Dynamics Simulations. *Pure Appl. Chem.* **1991**, *63*, 1743−1748.

(19) Kawska, A.; Brickmann, J.; Kniep, R.; Hochrein, O.; Zahn, D. An Atomistic Simulation Scheme for Modeling Crystal Formation from Solution. *J. Chem. Phys.* **2006**, *124*, 024513/1−024513/7.

(20) Mucha, M.; Jungwirth, P. Salt Crystallization from an Evaporating Aqueous Solution by Molecular Dynamics Simulation. *J. Phys. Chem. B* **2003**, *107*, 8271−8274.

(21) Zahn, D. Atomistic Mechanism for NaCl Nucleation from Aqueous Solution. *Phys. Rev. Lett.* **2004**, *92*, 040801/1−040801/4.

(22) Alejandre, J.; Hansen, J.-P. Ions in Water: From Ion Clustering to Crystal Nucleation. *Phys. Rev. E* **2007**, *76*, 061505/1−061505/5.

(23) Mendoza, F. N.; Alejandre, J. the Role of Ion−Water Interactions in the Solubility of Ionic Solutions. *J. Mol. Liq.* **2012**, DOI: 10.1016/j.molliq.2012.09.020.

(24) Berendsen, H. J. C.; Grigera, J. R.; Straatsma, T. P. The Missing Term in Effective Pair Potentials. *J. Phys. Chem.* **1987**, *91*, 6269−6271.

(25) Chandrasekhar, J.; Spellmeyer, D. C.; Jorgensen, W. L. Energy Component Analysis for Dilute Aqueous Solutions of Li^+, Na^+, F^-, and Cl^- Ions. *J. Am. Chem. Soc.* **1984**, *106*, 903−910.

(26) Åqvist, J. Ion−Water Interaction Potentials Derived from Free Energy Perturbation Simulations. *J. Phys. Chem.* **1990**, *94*, 8021−8024.

(27) Allen, M. P.; Tildesley, D. J. *Computer Simulation of Liquids*; Clarendon: Oxford, U.K., 1989.

(28) Berendsen, H. J. C.; van der Spoel, D.; van Drunen, R. GROMACS: A Message-Passing Parallel Molecular Dynamics Implementation. *Comput. Phys. Commun.* **1995**, *91*, 43−56.

(29) Hess, B.; Kutzner, C.; van der Spoel, D.; Lindahl, E. GROMACS 4: Algorithms for Highly Efficient, Load-Balanced, and Scalable Molecular Simulation. *J. Chem. Theory Comput.* **2008**, *4*, 435−447.

(30) Darden, T.; York, D.; Pedersen, L. Particle Mesh Ewald: An N−log(N) Method for Ewald Sums in Large Systems. *J. Chem. Phys.* **1993**, *98*, 10089−10092.

(31) Essmann, U.; Perera, L.; Berkowitz, M. L.; Darden, T.; Lee, H.; Pedersen, L. G. A Smooth Particle Mesh Ewald Method. *J. Chem. Phys.* **1995**, *103*, 8577−8592.

(32) Bussi, G.; Donadio, D.; Parrinello, M. Canonical Sampling through Velocity Rescaling. *J. Chem. Phys.* **2007**, *126*, 014101/1−014101/7.

(33) Berendsen, H. J. C.; Postma, J. P. M.; van Gunsteren, W. F.; DiNola, A.; Haak, J. R. Molecular Dynamics with Coupling to an External Bath. *J. Chem. Phys.* **1984**, *81*, 3684−3690.

(34) Hess, B.; Bekker, H.; Berendsen, H. J. C.; Fraaije, J. G. E. M. LINCS: A Linear Constraint Solver for Molecular Simulations. *J. Comput. Chem.* **1997**, *18*, 1463−1472.

(35) Aragones, J. L.; Sanz, E.; Vega, C. Solubility of NaCl in Water by Molecular Simulation Revisted. *J. Chem. Phys.* **2012**, *136*, 244508/1−1244508/16.

(36) Vega, C.; Abascal, J. L. F. Simulating Water with Rigid Non-Polarizable Models: A General Perspective. *Phys. Chem. Chem. Phys.* **2011**, *13*, 19663−19688.